HHS Public Access

Author manuscript

Nature. Author manuscript; available in PMC 2011 September 10.

Published in final edited form as:

Nature. 2011 March 10; 471(7337): 230–234. doi:10.1038/nature09855.

Using iPS cells to investigate cardiac phenotypes in patients with Timothy Syndrome

Masayuki Yazawa[1], **Brian Hsueh**[1,2], **Xiaolin Jia**[1,3], **Anca M. Pasca**[1,4], **Jonathan A. Bernstein**[4], **Joachim Hallmayer**[5], and **Ricardo E. Dolmetsch**[1]

[1] Department of Neurobiology, Stanford University School of Medicine, Stanford, California, U.S.A

[4] Department of Pediatrics, Stanford University School of Medicine, Stanford, California, U.S.A

[5] Department of Psychiatry & Behavioral Science, Stanford University School of Medicine, Stanford, California, U.S.A

Abstract

Individuals with congenital or acquired prolongation of the QT interval, or long QT syndrome (LQTS), are at risk of life threatening ventricular arrhythmia [1], [2]. LQTS is commonly genetic in origin but can also be caused or exacerbated by environmental factors[1], [3]. A missense mutation in the L-type calcium channel CaV1.2 leads to LQTS in patients with Timothy syndrome (TS)[4], [5]. To explore the effect of the TS mutation on the electrical activity and contraction of human cardiomyocytes (CMs), we reprogrammed human skin cells from TS patients to generate induced pluripotent stem cells (iPSCs), and differentiated these cells into CMs. Electrophysiological recording and calcium (Ca^{2+}) imaging studies of these cells revealed irregular contraction, excess Ca^{2+} influx, prolonged action potentials, irregular electrical activity and abnormal calcium transients in ventricular-like cells. We found that roscovitine (Ros), a compound that increases the voltage-dependent inactivation (VDI) of CaV1.2[6–8], restored the electrical and Ca^{2+} signaling properties of CMs from TS patients. This study opens new avenues for studying the molecular and cellular mechanisms of cardiac arrhythmias in humans, and provides a robust assay for developing new drugs to treat these diseases.

The risk of sudden death due to genetic and drug-induced LQTS is a major concern for patients, clinicians and pharmaceutical companies. Genetic LQTS has an estimated prevalence of 1 in 7,000 individuals and results from mutations in at least 10 genes[1], [4], [5], [9–12]. Drug-induced LQTS is a side effect of many approved drugs and is a common cause of drug failure in clinical trials. Despite our knowledge of many of the genes that cause LQTS,

Corresponding Author: Ricardo E. Dolmetsch, Department of Neurobiology, Stanford School of Medicine, 299 Campus Drive D227, Stanford, California 94305, USA, ricardo.dolmetsch@stanford.edu, Tel.: 650-723-9812, Fax: 650-725-3958.

[2]Present address: Department of Chemistry, Princeton University, Princeton, New Jersey, U.S.A.

[3]Present address: Baylor College of Medicine, Houston, Texas, U.S.A

Author Contributions:

M.Y. and R.E.D. designed research and wrote the manuscript; J.B., J.H. and R.E.D recruited the TS patients; M.Y. and K.J. generated and characterized control and TS iPSCs; A.M.P. conducted karyotyping; M.Y. performed generation and characterization of human cardiomyocytes and whole-cell patch clamp, Ca^{2+} imaging; M.Y. and B.H. analyzed CM contraction rates.

the mechanisms that underlie the disease in humans are incompletely understood. Mouse models of human LQTS have proved to be problematic because the mouse resting heart rate is approximately ten fold faster than that of humans and therefore mouse CMs have different electrical properties than their human counterparts. Therefore it is essential to develop models of LQTS that use human CMs.

CaV1.2 is the main L-type channel (LTC) in the mammalian heart and is essential for generating the cardiac action potential and for excitation contraction coupling[13, 14,17]. Ca^{2+} influx through LTCs in the plasma membrane causes Ca^{2+} release through ryanodine receptors (RyRs) in the sarcoplasmic reticulum (SR), leading to muscle contraction[14–16]. A single amino acid substitution in exon 8a of *CACNA1C*, the gene encoding CaV1.2 in humans, causes Timothy Syndrome (TS), a disorder characterized by LQTS, syndactyly (webbing of fingers and toes), immune deficiency, and autism[4]. Exon 8a is an alternatively spliced exon of CaV1.2, and the TS mutation is a G-R substitution that impairs inactivation of the channel [4, 5, 18, 19]. CaV1.2 channels undergo both voltage-dependent inactivation (VDI) and Ca^{2+}-dependent inactivation (CDI) and the G406R mutation severely impairs VDI and subtly affects CDI. Precisely how this leads to LQTS or arrhythmias in humans is not known.

To generate iPSCs from TS patients, we first obtained dermal fibroblasts from two patients by punch biopsy. We confirmed the presence of the TS mutation in these cells by sequencing the genomic DNA using two primer sets that recognize exon 8a in *CACNA1C* [4]. We next reprogrammed the fibroblasts to generate iPSCs using four retroviruses containing SOX2, OCT3/4, KLF4 and C-MYC[20, 21]. Three to four weeks after the infection, we picked human embryonic stem cell (hESC)-like colonies based on their morphology and expanded them for characterization and *in vitro* differentiation into cardiac cells (Fig. 1a). We generated a total 16 iPSC lines from two TS patients, and 10 control lines from two unrelated individuals without TS.

We selected five TS and five control iPSC lines for further characterization and generation of CMs (Supplementary Table 1). We used genomic sequencing to confirm that the TS iPSCs preserved the TS mutation (Supplementary Figure 1), and we mapped the integration sites of the retroviruses using nested PCR[22] (Supplementary Table 1). We found that all the lines had independent retroviral insertion sites and that the sites did not occur in the coding region of any gene. To examine whether the iPSC lines express human embryonic stem cell markers, we used immunocytochemistry (ICC) to look for NANOG and TRA2-49-6E (Alkaline Phosphatase) expression, and found that all of the lines expressed these markers (Supplementary Fig. 2). We also used RT-PCR to confirm that iPSCs expressed NANOG and REX1 and that they had silenced the exogenous genes that were used for reprograming (Supplementary Fig. 3). In addition, we performed genome wide microarray analyses of the cells and found that the gene expression patterns of iPSCs closely resembled those of hESCs and not of fibroblastsor neurons (GEO database http://www.ncbi.nlm.nih.gov/geo/query/acc.cgi?token=jncfzcucugewaha&acc=GSE25542). We also karyotyped the iPSC lines to ensure that they did not have large chromosomal abnormalities (Fig. 1b and Supplementary Table 1) and injected them into immuno-deficient mice to verify that they could generate teratomas. Both control and TS iPSCs were able to form tissues derived from all three germ

layers including neural tissues (ectoderm), cartilage (mesoderm) and gut-like epithelium (endoderm) (Supplementary Fig. 2 and Table 1) indicating that the iPSCs that we have generated are pluripotent.

To generate human CMs from iPSCs, we first prepared embryoid bodies (EBs) from five control and five TS iPSC lines. After one week in suspension culture (d7), we placed ~80 EBs onto gelatin-coated 100 mm dishes to allow EBs to attach. Thirty days (d37) after plating, we observed that ~0.5–20 % of the EBs showed rhythmic contractions (Fig. 1c). There were no significant differences in the number of contracting EBs formed from control and TS iPSC lines (data not shown). RT-PCR analysis revealed that the spontaneously contracting EBs expressed cardiac markers (Fig. 1d) and both exons 8 and 8A of *CAC-NA1C* but not *NANOG* indicating that these contain CMs but not iPSCs.

To examine the contractile properties of CMs we collected time-lapse images of spontaneously contracting EBs and analyzed their movement using image analysis software (Supplementary Movie 1–4 and Fig. 1e,f). We collected movies of 113 EBs derived from five TS iPSC lines and compared them to EBs derived from the five control lines. Control EBs contracted at approximately 60 bpm, similar to the resting heart rate in humans, while the TS CMs contracted at only ~30 bpm. Contraction of the TS EBs was significantly more irregular than contraction of control CMs (Fig. 1e,g). This was reflected in the broader distribution of inter-contraction intervals in TS EBs relative to those of controls (Fig. 1h). These results indicate that contracting EBs from multiple iPSC lines from both TS patients have disease specific defects.

To characterize the underlying defects in CMs from TS patients further, we dissociated contracting EBs into single cells. We stained these cells with antibodies that recognize the cardiac makers α-actinin, which is present at the Z-line of the sarcomere, and cardiac Troponin I, which is a cardiac-specific myofilament protein. More than 65% of the cells from the beating EBs expressed both proteins and had well-organized sarcomeres. There were no differences in the staining pattern of TS and control CMs. We next used whole-cell patch clamping to determine whether the TS mutation altered LTC VDI in human CMs. We measured LTC-generated currents using Ba^{2+} as the charge carrier and found that the LTC current in TS CMs had significantly reduced VDI compared to control cells (Fig. 2b–e and Supplementary Fig. 4). This was apparent both from the increased amplitude of the residual current after a 350ms depolarization and from increased current elicited by a 300 ms test pulse after a 2s depolarizing pulse to different voltages. In contrast, there was no difference between control and TS CMs in the current-voltage relationship or the peak amplitudes of Ba^{2+} currents (Fig. 2d). These results are broadly consistent with the properties of the TS mutant channel observed in heterologous expression systems[4, 18, 19].

Ca^{2+} influx through LTCs contributes to the plateau phase of the cardiac action potential (AP), so we asked whether the shape or duration of the AP in CMs was altered by the TS mutation. Using current-clamp recording, we examined spontaneous APs in control and TS CMs. Because human CM populations generated from iPSCs contain nodal-like, ventricular-like and atrial-like myocytes[23, 24], we harvested the mRNA from each patch-clamped CM and used single-cell RT-PCR of cardiac ventricular myosin light chain 2v (MLC2v,

Supplementary Fig. 5) to identify ventricular cells. We found that ventricular-like myocytes from TS patients had APs that were three times as long as those of control cells (Fig. 2f, g). In addition, the TS CMs exhibited a large number of depolarizing events that failed to trigger a full AP. These depolarizations were similar to the delayed after depolarizations (DADs) that arise following ectopic release of Ca^{2+} from the SR and which are associated with cardiac arrhythmias (Fig. 2f, h). In contrast we didn't find significant differences in the AP properties of nodal-like and atrial-like myocytes from control and TS patients (Supplementary Fig. 5). These suggest that ventricular CMs derived from TS iPSCs are defective and provides a possible cellular basis for LQTS and arrhythmia in these patients.

CaV1.2 channels play a crucial role in activating Ca^{2+}-induced Ca^{2+} release from the SR but the effect of altering CaV1.2 inactivation on this process is not known. We therefore asked how the TS mutation affects Ca^{2+} signaling in TS CMs. We used a confocal microscope to perform fast line-scan imaging of human CMs loaded with the Ca^{2+} indicator Fluo-4. The Ca^{2+} elevations in spontaneously contracting TS CMs were more irregular than those of control CMs (Fig. 3 and Supplementary Fig. 6). In addition, the TS mutation led to significantly larger and more prolonged Ca^{2+} elevations, indicating that channel inactivation is important for maintaining the timing and the amplitude of the ventricular AP.

The finding that CMs from TS patients have disease-specific electrical defects suggest that they might be a useful system for testing possible therapeutic compounds. As a proof of principle, we investigated whether Roscovitine (Ros), a cycline-dependent kinase inhibitor that increases VDI in HEK 293 cells expressing CaV1.2 channels[6–8], could rescue the phenotypes of TS CMs. We examined the effect of three different concentrations of Ros (10, 33.3 and 100 μM) on the timing and amplitude of spontaneous Ca^{2+} transients in TS CMs. Treatment with 100 μM Ros completely eliminated contractions but 33.3 μM Ros significantly reduced both the irregular timing and amplitude of Ca^{2+} transients (Fig. 4a,b and Supplementary Fig. 7). Washing out Ros partially restored the irregular Ca^{2+} transients in TS CMs but this effect did not reach significance [6–8].

To determine if Ros rescues the electrophysiological properties of TS CMs, we used whole-cell patch clamping to measure CaV1.2 currents and APs in TS CMs in the presence and absence of Ros. Ros significantly increased CaV1.2 VDI in TS CMs (Fig. 4c,d) but had only a mild effect on control CMs (Supplementary Fig. 8). Ros also reduced the duration of APs in TS CMs and decreased the frequency of abnormal depolarizing events (Fig. 4e,f). These results indicate that CMs from patients with LQTS can be used to screen potential drugs, and suggest that drugs related to Ros might be valuable tools for treating TS and other cardiac arrhythmias.

We have developed a new *in vitro* model for studying cardiac arrhythmias that has important advantages relative to existing approaches[25]. In contrast to mouse CMs, iPSC-derived EBs spontaneously contract at a rate that is similar to that of the human heart and single cells derived from these EBs have structural and electrical properties that are similar to those of CMs from human patients. Importantly, CMs derived from five different iPSC lines from two independent patients with LQTS had cellular defects that are consistent with the cardiac defects of the patients. The EBs from TS patients contracted slowly relative to control EBs

consistent with bradycardia in many TS patients. Ventricular CMs from TS patients also had prolonged APs that likely delay the repolarization of the heart and lead to LQTS. Both the isolated CMs and the EBs contracted arrhythmically and the CMs had frequent depolarizing events that failed to produce APs and were similar to DADs.

The phenotype of TS CMs stands in contrast to the phenotype of CMs from patients with LQTS1[12]. Only ventricular CM from TS had prolonged APs whereas both ventricular- and atrial-like CMs from LQTS1 had this phenotype. Furthermore, arrhythmias and delayed depolarizations were observed in spontaneously beating TS CMs whereas they could only be elicited in LQTS1 CM by stimulation with isoproterenol. While it is difficult to link these features to the Torsade de Points and to ventricular fibrillations in TS patients, these findings set the stage for the development of more sophisticated models of LQTS. Finally this study demonstrates that iPSC derived CMs are a useful platform for identifying drug candidates. Ros restored the AP duration in TS CMs and prevented the occurrence of arrhythmias. Even though Ros has other targets[26] it could be a useful lead compound for the development of new types of antiarrhythmics.

Summary of Methods

Control and TS iPSC lines were generated using retroviral infection with pMXs-SOX2, pMXs-OCT3/4, pMXs-MYC and pMXs-KLF4 expression plasmids (Add-gene) generated by Dr. Shinya Yamanaka's group[20]. The iPSCs were cultured on irradiated DR4 mouse embryonic fibroblast feeders using standard ES media with 10–15 ng/ml bFGF (R & D Systems), and cells were passaged with dispase (3 unit/ml, Invitrogen). The G1216A in exon 8a was detected by sequencing of PCR products from DNA harvested from fibroblasts and iPSC lines using primers for human Cav1.2 exon 8a. Immunocytochemistry, RT-PCR, microarray, karyotyping and teratoma formation assay were performed using standard protocols. For *in vitro* generation of cardiomyocytes, embryoid bodies were cultured with Wnt3a (100 ng/ml, R&D Systems) [27]. Whole-cell patch clamp recordings in single cardiomyocytes were conducted using standard methods. Live cell Ca^{2+} imaging was performed in single cardiomyocytes loaded with 5 μM Fluo-4 AM and 0.02% Pluronic F-127 (Molecular Probes) using fast line scanning (1.92 ms/line) on a confocal microscope (LSM 510 Meta, Carl Zeiss) with a 63× lens (NA=1.4). *R*-roscovitine was obtained from Sigma-Aldrich.

Supplementary Material

Refer to Web version on PubMed Central for supplementary material.

Acknowledgments

Katherine Timothy and the TS patients who participated in this study. Uta Francke for discussion and for providing karyotyping expertise; Athena Cherry and Dana Bangs for fibroblast isolation; K. C. Chan for iPSC cultures; O. Shcheglovitov for help with electrophysiological recordings; A. Olson for help with the confocal microscope. Funding was provided by grants from the Japan Society for the Promotion for Science and the American Heart Association Western States to M.Y., and a National Institutes of Health Director's Pioneer Award, a grant from the Simons Foundation to R.E.D and gifts from Mrs. Linda Miller, Ben and Felicia Horowitz and Mr. and Mrs. Michael McCafferey.

References

1. Keating MT. The long QT syndrome. A review of recent molecular genetic and physiologic discoveries. Medicine (Baltimore). 1996; 75:1–5. [PubMed: 8569466]
2. Huikuri HV, Castellanos A, Myerburg RJ. Sudden death due to cardiac arrhythmias. N Engl J Med. 2001; 345:1473–1482. [PubMed: 11794197]
3. Paakkari I. Cardiotoxicity of new antihistamines and cisapride. Toxicol Lett. 2002; 127:279–284. [PubMed: 12052668]
4. Splawski I, et al. Ca(V)1.2 Ca^{2+} channel dysfunction causes a multisystem disorder including arrhythmia and autism. Cell. 2004; 119:19–31. [PubMed: 15454078]
5. Splawski I, et al. Severe arrhythmia disorder caused by cardiac L-type Ca^{2+} channel mutations. Proc Natl Acad Sci U S A. 2005; 102:8089–8096. discussion 8086–8088. [PubMed: 15863612]
6. Yarotskyy V, Elmslie KS. Roscovitine, a cyclin-dependent kinase inhibitor, affects several gating mechanisms to inhibit cardiac L-type (Ca(V)1.2) Ca^{2+} channels. Br J Pharmacol. 2007; 152:386–395. [PubMed: 17700718]
7. Yarotskyy V, Gao G, Peterson BZ, Elmslie KS. The Timothy syndrome mutation of cardiac CaV1.2 (L-type) channels: multiple altered gating mechanisms and pharmacological restoration of inactivation. J Physiol. 2009; 587:551–565. [PubMed: 19074970]
8. Yarotskyy V, et al. Roscovitine binds to novel L-channel (CaV1.2) sites that separately affect activation and inactivation. J Biol Chem. 2010; 285:43–53. [PubMed: 19887376]
9. Roden DM, Viswanathan PC. Genetics of acquired long QT syndrome. J Clin Invest. 2005; 115:2025–2032. [PubMed: 16075043]
10. Chen L, et al. Mutation of an A-kinase-anchoring protein causes long-QT syndrome. Proc Natl Acad Sci U S A. 2007; 104:20990–20995. [PubMed: 18093912]
11. Roden DM. Clinical practice. Long-QT syndrome. N Engl J Med. 2008; 358:169–176. [PubMed: 18184962]
12. Moretti A, et al. Patient-Specific Induced Pluripotent Stem-Cell Models for Long-QT Syndrome. N Engl J Med. 2010
13. Reuter H. Ion channels in cardiac cell membranes. Annu Rev Physiol. 1984; 46:473–484. [PubMed: 6324658]
14. Flucher BE, Franzini-Armstrong C. Formation of junctions involved in excitation-contraction coupling in skeletal and cardiac muscle. Proc Natl Acad Sci U S A. 1996; 93:8101–8106. [PubMed: 8755610]
15. Takeshima H, et al. Embryonic lethality and abnormal cardiac myocytes in mice lacking ryanodine receptor type 2. EMBO J. 1998; 17:3309–3316. [PubMed: 9628868]
16. Yazawa M, et al. TRIC channels are essential for Ca^{2+} handling in intracellular stores. Nature. 2007; 448:78–82. [PubMed: 17611541]
17. Seisenberger C, et al. Functional embryonic cardiomyocytes after disruption of the L-type alpha1C (Cav1.2) Ca^{2+} channel gene in the mouse. J Biol Chem. 2000; 275:39193–39199. [PubMed: 10973973]
18. Barrett CF, Tsien RW. The Timothy syndrome mutation differentially affects voltage- and calcium-dependent inactivation of CaV1.2 L-type Ca^{2+} channels. Proc Natl Acad Sci U S A. 2008; 105:2157–2162. [PubMed: 18250309]
19. Thiel WH, et al. Proarrhythmic defects in Timothy syndrome require calmodulin kinase II. Circulation. 2008; 118:2225–2234. [PubMed: 19001023]
20. Takahashi K, et al. Induction of pluripotent stem cells from adult human fibroblasts by defined factors. Cell. 2007; 131:861–872. [PubMed: 18035408]
21. Yu J, et al. Induced pluripotent stem cell lines derived from human somatic cells. Science. 2007; 318:1917–1920. [PubMed: 18029452]
22. Aoi T, et al. Generation of pluripotent stem cells from adult mouse liver and stomach cells. Science. 2008; 321:699–702. [PubMed: 18276851]

23. He JQ, Ma Y, Lee Y, Thomson JA, Kamp TJ. Human embryonic stem cells develop into multiple types of cardiac myocytes: action potential characterization. Circ Res. 2003; 93:32–39. [PubMed: 12791707]

24. Zhang J, et al. Functional cardiomyocytes derived from human induced pluripotent stem cells. Circ Res. 2009; 104:e30–41. [PubMed: 19213953]

25. Brunner M, et al. Mechanisms of cardiac arrhythmias and sudden death in transgenic rabbits with long QT syndrome. J Clin Invest. 2008; 118:2246–2259. [PubMed: 18464931]

26. Meijer L, et al. Biochemical and cellular effects of roscovitine, a potent and selective inhibitor of the cyclin-dependent kinases cdc2, cdk2 and cdk5. Eur J Biochem. 1997; 243:527–536. [PubMed: 9030781]

27. Tran TH, et al. Wnt3a-induced mesoderm formation and cardiomyogenesis in human embryonic stem cells. Stem Cells. 2009; 27:1869–1878. [PubMed: 19544447]

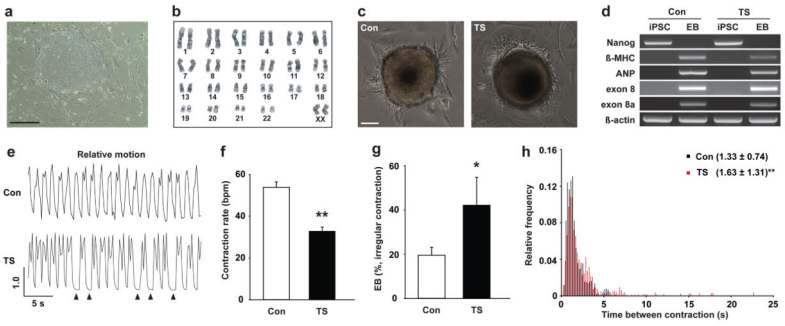

Figure 1. Generation of cardiomyocytes from control and TS iPSCs

a) Phase contrast images of iPSC line (9862-61) derived from a TS patient. Scale bar, 400 μm. b) Karyogram of TS iPSCs (7643-5). c) Images of spontaneously contracting embryoid bodies (EBs) generated from control (Con, left) and TS iPSCs (right). Scale bar, 100 μm. d) Examination of pluripotent and cardiac gene expression using RT-PCR with primer sets for pluripotent gene (NANOG), cardiac markers (β-MHC and ANP), CaV1.2 channels (exon 8 and 8a) and house keeping gene (β-actin). e) Relative motion of contracting control and TS EBs. Arrowheads show missing contractions. f) Contraction rate of TS and control EBs (control, *n*=85 EBs in 5 lines; TS, *n*=113 in 5 lines, mean ± s.e.m.). g) Fraction of TS and control EBs showing arrhythmic contractions (control, *n*=5 lines, 85 EBs; TS, *n*=5 lines, 113 EBs, mean ± s.e.m.). h) Histogram of inter-contraction intervals for control EBs (black column, *n*=3,241 contractions in 5 lines) and TS EBs (red column, *n*=3,998 in 5 lines, mean ± s.d.). Statistical analyses were conducted using Student's t-test (**P*<0.05, ***P*<0.01).

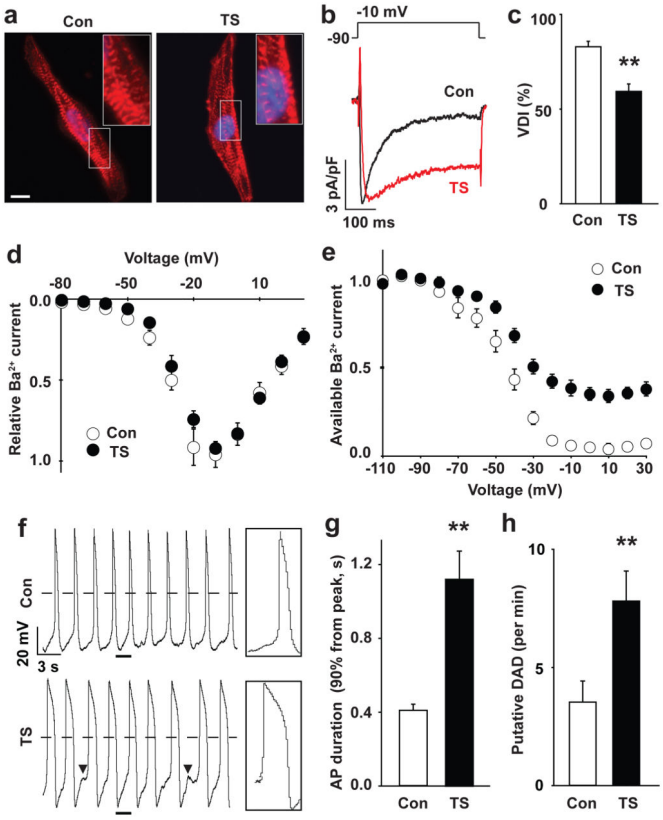

Figure 2. Electrophysiological features of TS cardiomyocytes

a) Immunocytochemistry of human cardiomyocytes (CMs) generated from control (left) and TS iPSCs (right) using anti-α-Actinin antibodies (red). The nuclei (blue) are marked by Hoechst staining. Insets show high magnification images of the sarcomeres. Scale bar, 10 μm. b) Voltage-clamp recording of Ba^{2+} currents in control (black) and TS (red) CMs show a defect in voltage-dependent channel inactivation (VDI) following a voltage pulse from −90 to −10 mV. c) VDI in control and TS CMs 350 ms after the start of the pulse (**P<0.01; students T test). d) The IV relationship of TS (●) and control (○) Ca^{2+} currents (mean ± s.e.m.) are statistically identical. There were no significant differences in the peak amplitude of Ba^{2+} currents between control and TS CMs (data not shown). e) Ba^{2+} current in control and TS myocytes stimulated with a test pulse to +10 mV following a family of prepulses from −110 to +30 mV in 10 mV increments (raw traces in Supplementary Fig. 4c, control, n=23 cells in 4 lines; TS, n=19 in 4 lines, mean ± s.e.m.). f) Spontaneous action potentials (AP) in control and TS ventricular-like myocytes measured in current-clamp mode. Boxes show the regions indicated by underlines at an expanded time scale. Arrowheads show putative delayed afterdepolarizations (DADs). Dashed lines show 0 mV. g) AP duration in TS and control ventricular CMs. The expression of the ventricular marker, MLC2v, was confirmed with single-cell RT-PCR immediately after whole-cell patch recording (Supplementary Fig. 5). h) Putative DADs in TS and control ventricular-like cardiomyocytes (control, n=22 cells in 4 lines; TS, n=14 in 4 lines, mean ± s.e.m.). Statistical analyses were performed with Student's t-test (**P<0.01).

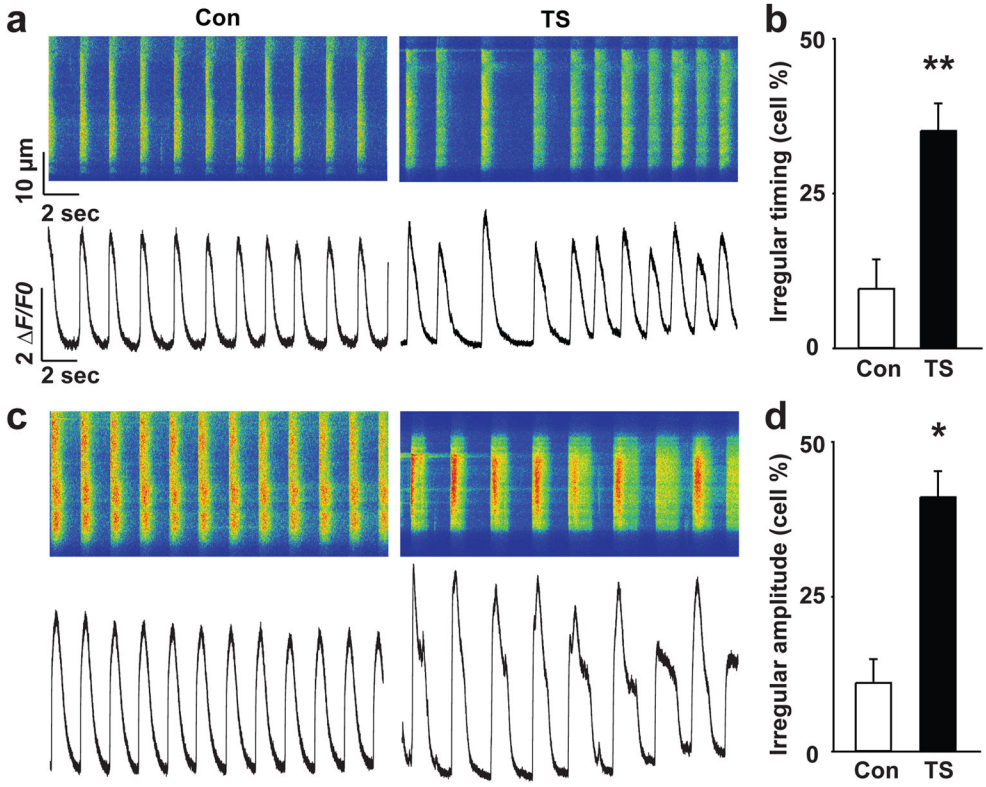

Figure 3. Ca^{2+} signaling in TS and control cardiomyocytes

Representative line-scan images (a, c, top) and spontaneous Ca^{2+} transients (a, c, bottom) in control (left) and TS CMs (right). TS CMs showed more irregular timing (b) and amplitude (d) of spontaneous Ca^{2+} transients compared to control cells (see Supplementary Fig. 6 and Methods for details about the analysis, control, n=102 cells in 4 lines; TS, n=149 in 4 lines, mean ± s.e.m.; *P<0.05, **P<0.01., students T-test).

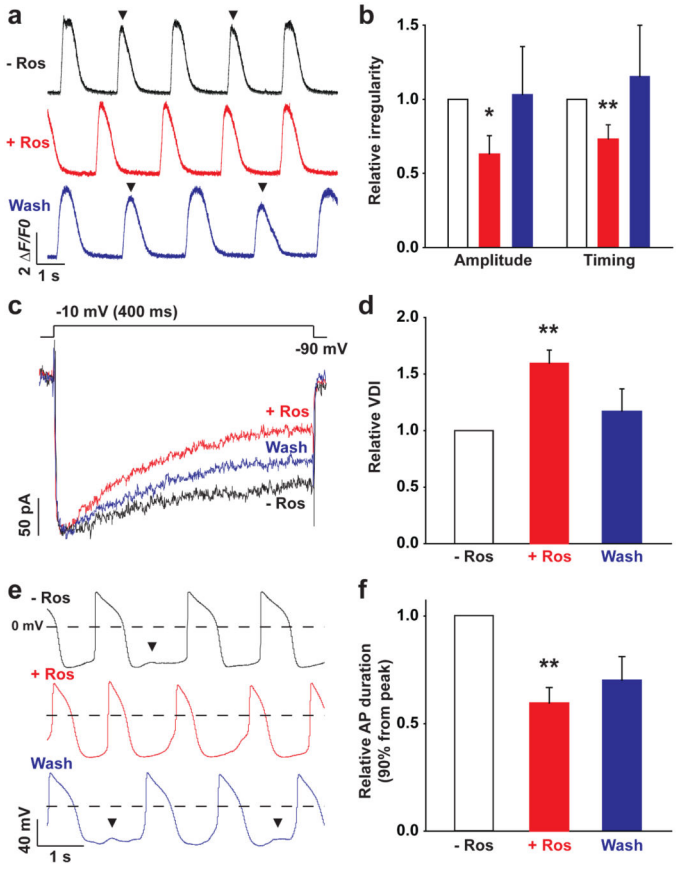

Figure 4. Roscovitine rescues the cellular phenotypes of TS cardiomyocytes

a) Spontaneous Ca^{2+} transients in TS CMs before (black) and after treatment with 33.3 μM Ros (red) as well as after wash out (blue). Arrowheads show irregular Ca^{2+} elevations. b) Effects of Ros on the relative irregularity of the amplitude and timing of the spontaneous Ca^{2+} transients in TS CMs (*n*=8 cells in 2 lines, **P*<0.05, ***P*<0.01). c) Ba^{2+} currents in TS CMs recorded in voltage-clamp mode before (black) during (red) and after (blue) treatment with 33.3 μM Ros. Ros promoted inactivation of currents in TS CMs. d) Effects of Ros on CaV1.2 VDI in CMs (*n*=5 cells in 2 lines, ***P*<0.01). e) Spontaneous APs recorded in current-clamp recording before, during and after treatment with Ros. Arrowheads show putative DADs. f) Ros prevented AP prolongation observed in TS CMs (*n*=8 cells in 2 lines, ***P*<0.01, mean ± s.e.m.).